A quantitative assessment of the production of _OH and additional oxidants in the dark Fenton reaction: Fenton degradation of aromatic amines

A quantitative assessment of the production of •OH and additional oxidants in the dark Fenton reaction: Fenton degradation of aromatic amines

Claudio Minero *, Mirco Lucchiari, Valter Maurino, Davide Vione *

Received (in XXX, XXX) Xth XXXXXXXXX 20XX, Accepted Xth XXXXXXXXX 20XX
DOI: 10.1039/b000000x

This paper reports the results of a kinetic study into the transformation of 2,4- and 3,4-dichloroaniline (2,4-DCA, 3,4-DCA) and of methyl yellow (MY) with the Fenton reagent in aqueous solution. All the substrates can be degraded in the presence of Fe(II) + H_2O_2, but the reaction between Fe(II) and H_2O_2 causes substrate degradation and Fe(II) oxidation within seconds under the adopted conditions. The HPLC, GC-MS and IC analyses only allow the monitoring of the reaction after all Fe(II) has been consumed, when degradation proceeds more slowly via Fe(III) reduction to Fe(II). Substrate degradation in the first part of the reaction was studied by stopped-flow spectrophotometry, using MY as substrate. The results are consistent with a reaction involving •OH, where both Fe(II) and H_2O_2 compete with MY for the hydroxyl radical. However, the experimental data indicate that •OH is unlikely to be the only product of the reaction between Fe(II) and H_2O_2. Another species, possibly the ferryl ion (FeO^{2+}) is formed as well but has a negligible role in MY degradation. The Fenton reaction would thus yield both •OH (about 60% at pH 2) and ferryl (about 40%), and the 60:40 branching ratio between •OH and the other species is compatible with additional data here reported concerning the degradation of 2,4-DCA and 3,4-DCA in the first ferrous step of the Fenton reaction. The reported findings will hopefully indicate a way out of a long-lasting controversy concerning the mechanism of the Fenton process, also suggesting an approach to quantitatively determine the formation yields of the reactive species as well as a strategy to identify the reactant that is actually involved in substrate transformation.

Introduction

The most common interpretation of the mechanism of the Fenton reaction is traditionally based on the proposal by Haber and Weiss and further modifications.[1] According to that traditional view, the key process is the generation of hydroxyl radicals upon reaction between Fe(II) and H_2O_2. More recently a controversy has appeared concerning the nature of the oxidising species, which questioned the role and sometimes even the occurrence of •OH. Indeed, the Fenton reaction is sometimes different from the expected behaviour of homogeneous •OH.[2,3] The possible role of high-valence iron species has been proposed (usually indicated as ferryl), in analogy with some Fenton-like processes that involve Fe(II) complexes with organic ligands and different peroxides than H_2O_2, such as $Fe^{II}L_x$ + HOOH or $Fe^{II}L_x$ + ROOH.[4,5] The problem is certainly very difficult because, if additional oxidants are formed in the Fenton reaction, in aqueous solution they would mimic the reactivity of •OH and produce interference even with otherwise selective techniques such as the EPR spin trapping.[6,7]

A large mount of evidence has recently been provided in favour of ferryl, which has also been isolated and identified,[8-14] although its actual involvement in Fenton degradation is still questioned.[15] A reasonable interpretation of the literature findings is that both •OH and ferryl are formed by Fe(II) + H_2O_2, with variable yields depending on pH. In particular, the •OH yield would decrease with increasing pH and the opposite would happen with ferryl.[16] On the other hand, extensive kinetic studies and kinetic modelling have been carried out successfully based on the classical interpretation of the Fenton process, considering not only the production of key oxidising species but also the many subsequent reactions that take place in solution.[17-19]

The Fenton reaction is frequently studied because it is one of the most widely applied Advanced Oxidation Processes for water and wastewater decontamination,[20] due to its effectiveness in the degradation of many organic compounds.[21-30] In the Fenton treatment, Fe(II) can be added as such (dark process), or photochemically generated upon photolysis of dissolved Fe(III) (photo-Fenton reaction)[31-33] or suspended Fe(III) (hydr)oxides.[34]

$$Fe^{III}\text{-}L + h\nu \rightarrow Fe^{2+} + L^{+\bullet} \qquad (1)$$

Other techniques (electro-Fenton, sono-Fenton) to produce Fe(II) from Fe(III) are also possible, although they are less widely applied than the photochemical variant.[35,36]

In this work we report on the Fenton degradation of aromatic amines, which allowed the quantification of the relative role of •OH and other oxidants (*e.g.* ferryl) in the process. The fast reaction between Fe^{2+} and H_2O_2 was studied by use of the stopped-flow technique and with an amine dye (methyl yellow) as substrate. Considerations suggested by the stopped-flow study were further confirmed by the degradation of dichloroanilines, monitored by HPLC. This technique gave insight both into the substrate fraction that was degraded in the first reaction step (Fe^{2+} + H_2O_2), and into the following steps that are dominated by the reduction of Fe(III).

Experimental

Chemicals

2,4-Dichloroaniline (purity grade 99%), 3,4-dichloroaniline (98%), 2,4-dichlorophenol (99%), 3,4-dichlorophenol (99%), methyl yellow, methanesulphonic acid (>99.5%), $NaHCO_3$ (>99.7%), and NH_4Cl (98%) were purchased from Aldrich, dichloromethane (for gas chromatography), 2-propanol (gradient grade for liquid chromatography), $FeSO_4 \cdot 7\ H_2O$ (99.5%), $NaH_2PO_4 \cdot H_2O$ (>99%), $Na_2HPO_4 \cdot 2\ H_2O$ (>99.5%), K_2CO_3 (>99.5%), H_2O_2 (35%), H_2SO_4 (96%), and NaCl (99.5%) from VWR Int., acetonitrile (gradient grade) from Carlo Erba, anhydrous Na_2SO_4 (>99.5%,) from ProLabo. $FeSO_4 \cdot 7\ H_2O$ was purified by recrystallisation, the other reagents were used as received without further purification.

Instrumentation and procedures

The Fenton reaction was studied in aqueous solution. The degradation of methyl yellow (MY) at pH 1.8 by H_2SO_4 was assessed with the stopped-flow technique. The different reactants (substrate + H_2SO_4 + $FeSO_4$, H_2O_2 + H_2SO_4) were mixed by means of two syringes. The degradation of the dichloroanilines at pH 2.0 by H_2SO_4 (and of MY at pH 1.8 to detect the transformation intermediates) was carried out in 100 mL beakers under magnetic stirring. The different reagents were added from separate stock solutions and the last addition was of H_2O_2 to start the reaction. At selected time intervals, aliquots were withdrawn for successive analysis by HPLC, IC or GC-MS.

HPLC analyses were carried out with a Merck-Hitachi chromatograph, equipped with a Rheodyne injector (loop volume 54 μL), model L-6200 and L-6000 pumps for high-pressure gradients, a 125 × 4 mm RP-C18 LiChroCART column (VWR) packed with LiChrospher 100 RP-18 (particle diameter 5 μm), and a model L-4200 UV-Vis detector. The injected samples were eluted with a 40/60 mixture of acetonitrile/aqueous phosphate buffer (NaH_2PO_4 + Na_2HPO_4, total phosphate 0.050 M, pH 7.5) at 1.0 mL min^{-1} flow rate, and detected at 240 nm. The retention times were [min]: 2,4-dichloroaniline (2,4-DCA) [11.00], 3,4-dichloroaniline (3,4-DCA) [8.80], 2,4-dichlorophenol (2,4-DCP) [6.80], 3,4-dichlorophenol (3,4-DCP) [7.95].

IC analyses were carried out with a Dionex DX 500 ion chromatograph, equipped with Rheodyne injector (loop volume 50 μL), LC 30 chromatography oven, GP 40 gradient pump, and ED 40 electrochemical detector (conductivity mode). Analyses for the anions made use of a Dionex Ion Pac AG9-HC 4 × 50 mm guard column, Ion Pac AS9-HC 4 × 250 mm column, and Ion Pac ASRS-ULTRA 4 mm conductivity suppressor. Elution was carried out with a solution containing 4.75×10^{-3} M $NaHCO_3$ and 1.14×10^{-2} M K_2CO_3. Cation analyses made use of a Dionex Ion Pac CG12A 4 × 50 mm guard column, Ion Pac CS12A 4 × 250 mm column, and Ion Pac CSRS-ULTRA 4 mm conductivity suppressor. Samples were eluted with a solution containing 2.5×10^{-2} M CH_3SO_3H. In both cases the flow rate was 1.0 mL min^{-1}. Under the respective conditions the retention times were [min]: chloride [5.60], nitrate [9.70], ammonium [4.15].

Aliquots for GC-MS analysis were treated with excess Na_2SO_4 and extracted with dichloromethane. The extract was dried with anhydrous Na_2SO_4 and concentrated under a gentle stream of high-purity nitrogen. Dichloromethane extracts were injected into a Hewlett Packard 6890 Met GC-MS, equipped with a phenylmethylsilicone capillary column (HP 5MS, length 30 m, i.d. 0.25 mm, film thickness 0.25 μm) and a HP 5973 mass detector (EI-SCAN mode). The following conditions were used: manual splitless injection (1 μL volume), gas carrier (He) flow rate 1 mL min^{-1}, injector temperature 300°C, column temperature from 70°C (3 min) to 300 °C at 10°C min^{-1}. Under such conditions the retention times were [min]: 2,4-DCA [15.10], 2,4-DCP [12.40], 2,4,6-trichloroaniline [16.00], 2-chloro-1,4-benzoquinone [10.95].

The stopped-flow measures were carried out with a Hi-tech stopped-flow spectrophotometer composed of a SF-3L support unit, equipped with a temperature-control device (set at 25° C) and a SF-40C control unit. The spectrophotometer was equipped with Hi-tech arc lamp and MG-10 grating monochromator. Data acquisition was performed with an Agilent Infiniium oscilloscope (500 MHz, 1 GSa s^{-1}).

UV-Vis spectra were obtained with a Varian CARY 100 Scan double-beam UV-Vis spectrophotometer, using Hellma 104-QS quartz cuvettes (1.000 cm optical path length). The solution pH was measured with a combined glass electrode connected to a Metrohm 713 pH-meter. Water used for the experiments was of Milli-Q quality.

Results and discussion

The reaction between Fe^{2+} and H_2O_2 is relatively fast,[37-39] thus the related degradation of substrates cannot be properly monitored by liquid chromatography unless very low concentrations of the reactants are used. The stopped-flow technique is suitable to study fast processes but it cannot be coupled with separation devices. With our stopped-flow instrument the monitoring can be carried out spectrophotometrically, and the choice of a substrate absorbing visible radiation is needed to minimise spectral interference. Azo dyes such as MY are a reasonable choice, because the –N=N– group is very reactive and its cleavage or transformation causes a loss of conjugation and, therefore, the disappearance of the band that absorbs visible radiation.[40]

Degradation of methyl yellow

Experimental data. Methyl yellow (MY) is an azo dye (N,N-dimethyl-4-(phenylazo)aniline) that undergoes acid-base equilibrium. Its absorption spectrum at different pH values shows the presence of an isosbestic point at 471 nm (see Figure 1). At this wavelength these is no spectral interference by the Fenton reagent, thus we carried out the stopped-flow runs at 471 nm.

Experiments were carried out at pH 1.8, where practically all MY is protonated as suggested by Figure 1. A preliminary study of the transformation intermediates was carried out with aqueous saturated solutions of MY in the presence of 1 mM Fe(II) + 1 mM H_2O_2 at pH 1.8 and 25°C. The reaction was quenched at different time intervals with a phosphate buffer at pH 7.0 (total phosphate concentration 0.10 M), which also deprotonated MY and related compounds. After addition of Na_2SO_4, the solution was extracted with dichloromethane and the organic phase was analysed by GC-MS. The dichloromethane used for the extraction and CH_2Cl_2-extracted Milli-Q water were adopted as analytical blanks. The main detected intermediates are derivatives resulting

from oxidative attack on the azo group (see Scheme 1).

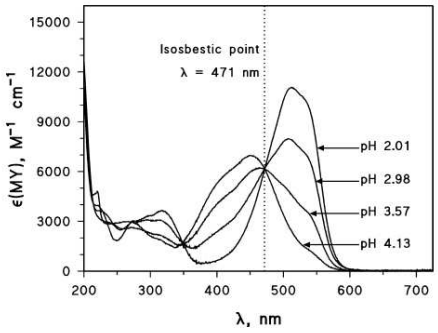

Figure 1. Absorption spectra (molar absorption coefficients ε) of MY at different pH values in aqueous solution. The isosbestic point at 471 nm is highlighted.

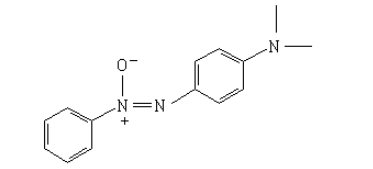

N,N-Dimethyl-4-(phenyl-ONN-azoxy)aniline

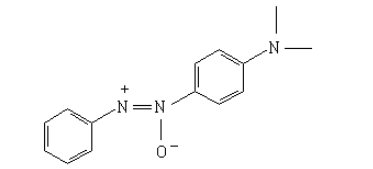

N,N-Dimethyl-4-(phenyl-NNO-azoxy)aniline

Scheme 1. Early transformation intermediates of MY by the Fenton reagent (1 mM Fe(II) + 1 mM H_2O_2, pH 1.8, GC-MS analysis).

Oxidative cleavage of the –N=N– group is likely to be the main reaction pathway, as confirmed by the detection of many compounds clearly originating from such a cleavage (N,N-dimethyl-4-nitroaniline, N,N-dimethylaniline, aniline, 3-(N,N-dimethylamino)phenol, 4-aminophenol, phenol, and 1,3-dihydroxyphenol). The presence of many hydroxylated aromatics (phenolic compounds) is consistent with a relevant role played by $^{\bullet}OH$ in the Fenton degradation of MY, though not constituting compelling evidence in its favour.

Figure 2 reports the time evolution of 10 μM MY (decimal logarithm of the absorbance as a function of time) in the presence of 1 mM Fe(II), in aqueous solution at pH 1.8 adjusted by addition of H_2SO_4, for different values of $[H_2O_2]$ (varied in the range of 0.8 - 30 mM). The disappearance of MY, monitored by stopped-flow spectrophotometry, was practically complete before the expected total consumption of Fe(II). Based on kinetic data reported in the literature,[37-39] the concentration of Fe(II) is expected to be halved in a time varying from 0.5 s with 30 mM H_2O_2 to ~20 s with 0.8 mM H_2O_2. The disappearance of MY down to ~1/20 of the initial concentration requires a shorter time (see Figure 3). Therefore, MY degradation is mostly accounted for by the reaction between Fe(II) and H_2O_2, with a negligible role of the following ferric step (reactions (2-4)).[17,18]

$$Fe(III) + H_2O_2 \rightarrow Fe(II) + HO_2^{\bullet} + H^+ \quad (2)$$
$$Fe(III) + HO_2^{\bullet} \rightarrow Fe(II) + O_2 + H^+ \quad (3)$$
$$Fe(III) + O_2^{-\bullet} \rightarrow Fe(II) + O_2 \quad (4)$$

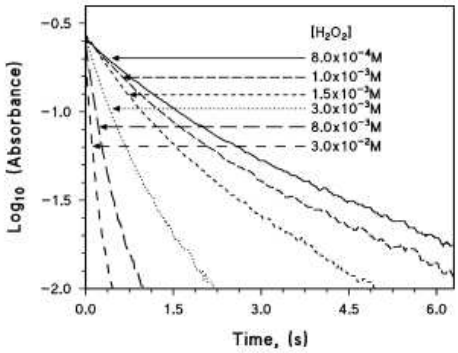

Figure 2. Time trend of the 471 nm absorbance (decimal logarithm) for the degradation of 10 μM MY in the presence of 1 mM Fe(II) in aqueous solution (the initial $[H_2O_2]$ is reported on the Figure). pH 1.8 by addition of H_2SO_4, reaction temperature 25°C.

Kinetic data treatment. A simplified kinetic model can be elaborated to account for MY degradation by the Fenton reagent, based on a free radical mechanism [37] where the key oxidant is $^{\bullet}OH$ (mechanism A, reactions 5, 6, 7a-10a). Alternatively, these reactions could be replaced by a non-radical mechanism [38,39] that implies the participation of the ferryl ion (here indicated as FeO^{2+}; mechanism B, reactions 5, 6, 7b-10b). The formation of a reactive complex between Fe(II) and H_2O_2 is hypothesised,[38,39,41] which can evolve into $^{\bullet}OH$ or FeO^{2+}. Note that both oxidants could react with either Fe^{2+}, H_2O_2 or MY:

$$Fe^{2+} + H_2O_2 \rightarrow \{Fe^{2+}\text{-}H_2O_2\} \quad [k_1] \quad (5)$$
$$\{Fe^{2+}\text{-}H_2O_2\} \rightarrow Fe^{2+} + H_2O_2 \quad [k_2] \quad (6)$$

Mechanism A

$$\{Fe^{2+}\text{-}H_2O_2\} + H^+ \rightarrow {}^{\bullet}OH + Fe^{3+} + H_2O \quad [k_{3a}] \quad (7a)$$
$$^{\bullet}OH + Fe^{2+} + H^+ \rightarrow Fe^{3+} + H_2O \quad [k_{Ba}] \quad (8a)$$
$$^{\bullet}OH + H_2O_2 \rightarrow HO_2^{\bullet} + H_2O \quad [k_{Ca}] \quad (9a)$$
$$^{\bullet}OH + MY \rightarrow MY_{ox} \quad [k_{Da}] \quad (10a)$$

Mechanism B

$$\{Fe^{2+}\text{-}H_2O_2\} \rightarrow FeO^{2+} + H_2O \quad [k_{3b}] \quad (7b)$$
$$FeO^{2+} + Fe^{2+} + 2\,H^+ \rightarrow 2\,Fe^{3+} + H_2O \quad [k_{Bb}] \quad (8b)$$
$$FeO^{2+} + H_2O_2 \rightarrow Fe^{2+} + O_2 + H_2O \quad [k_{Cb}] \quad (9b)$$
$$FeO^{2+} + MY \rightarrow MY_{ox} \quad [k_{Db}] \quad (10b)$$

The analogies between mechanism A and B only hold for the fast step of the Fenton process, but there are different kinetic implications for the following steps. Actually, in mechanism A the Fe(III) would be reduced back to Fe(II), while the ferryl ion could react with Fe^{3+} to form $FeOFe^{5+}$, for which the reduction to Fe(II) is rather slow.[38] However, these late processes would not affect the reaction studied by stopped flow.

An additional issue is that pH was adjusted by addition of H_2SO_4 and Fe(II) was added in the form of $FeSO_4$, thus part of $^{\bullet}OH$ formed in reaction (7a) would react with HSO_4^- (rate constant 1.2×10^6 M^{-1} s^{-1} [42]). However, considering the rate constants of reactions (8a) (4.0×10^8 M^{-1} s^{-1}, [42]) and (9a) (2.7×10^7

M^{-1} s^{-1}, [42]) and the concentrations of Fe(II) and H_2O_2, the reaction between $^{\bullet}OH$ and HSO_4^- can be neglected.

In the hypothesis that MY degradation takes place exclusively upon reaction with either $^{\bullet}OH$ (mechanism A) or FeO^{2+} (mechanism B), the application of the steady-state approximation to the concentration of the reactive specie R ($^{\bullet}OH$ or FeO^{2+}) yields the following equation:

$$-\frac{\partial[MY]}{\partial t} = k_D \cdot [R]_{steady\text{-}state} \cdot [MY] \qquad (11)$$

where

$$[R]_{steady-state} = \frac{k_A \cdot [Fe(II)] \cdot [H_2O_2]}{k_B \cdot [Fe(II)] + k_C \cdot [H_2O_2] + k_D \cdot [MY]} \qquad (12)$$

and $k_A = \frac{k_1 \cdot k_3}{k_2 + k_3}$ [38] is the observed rate constant for Fe(II) consumption ($k_3 = k_{3a}$ or k_{3b}). The choice of the rate constant (*e.g.* k_{Da} or k_{Db} for k_D) depends on the actual mechanism (A or B) that is operational. Within this approach, the two mechanisms are considered as mutually exclusive.

The differential equation (11,12) has no analytical solution if [Fe(II)], $[H_2O_2]$ and [MY] are functions of time. To obtain a solution one can focus on the initial rates, for which [Fe(II)] ≈ $[Fe(II)]_o$ and $[H_2O_2] \approx [H_2O_2]_o$. As we monitored the time evolution of MY, the analytical function [MY](t) cannot be obtained unless the term k_D [MY] is neglected in the denominator of eq. (12), in which case the degradation of MY follows a pseudo-first order kinetics. Under this approximation, the plots of $Log_{10}(A)$ *vs.* time should be linear. Figure 2 indicates that the pseudo-first order approximation is valid only in the initial part of the curves, thus some errors might derive from the time interval chosen for the fit. Numerical simulations suggested that if [MY](t) varies by no more than 10% of its initial value, the error associated to the pseudo first-order approximation is below 3-5%. This is comparable with data reproducibility (around 5%). Under the cited approximation the time evolution of MY absorbance is $A_t = A_o\, e^{-k_{obs}\, t}$, where A_o is the initial absorbance (0.27 for 10 μM MY), *t* the time in seconds, and k_{obs} the observed pseudo-first order rate constant (s^{-1}). The initial degradation rate of MY (r_o) is given by $r_o = k_{obs} \times [MY]_o$.

Under the approximations [Fe(II)] ≈ $[Fe(II)]_o$, $[H_2O_2] \approx [H_2O_2]_o$ and [MY] ≈ $[MY]_o$, and considering the initial rate r_o, equations (11,12) can be linearised as follows:

$$r_o^{-1} = \frac{k_B}{k_A k_D [H_2O_2]_o [MY]_o} + \frac{k_C}{k_A k_D [Fe(II)]_o [MY]_o} + \frac{1}{k_A [Fe(II)]_o [H_2O_2]_o} \qquad (13)$$

Based on equation (13) and on stopped-flow experiments where $[Fe(II)]_o$ was varied between 1 and 5 mM, it is possible to obtain the plots of r_o^{-1} *vs.* $[Fe(II)]_o^{-1}$ and r_o^{-1} *vs.* $[H_2O_2]_o^{-1}$. The former plots are shown in Figure 3 and their linearity is fully compatible with equation (13). Note that the dashed lines of Figure 3 are not regression ones: their meaning will be explained later. The plots of r_o^{-1} *vs.* $[H_2O_2]_o^{-1}$ (not shown) were linear as well.

Equation (13) is the starting point to obtain the values of the kinetic constants. The plot of r_o^{-1} *vs.* $[Fe(II)]_o^{-1}$ is a line with slope $S_1 = \{k_C\, k_A^{-1}\, k_D^{-1}\, [MY]_o^{-1} + k_A^{-1}\, [H_2O_2]_o^{-1}\}$ and intercept $I_1 = \{k_B\, k_A^{-1}\, k_D^{-1}\, [MY]_o^{-1}\, [H_2O_2]_o^{-1}\}$. Furthermore, by plotting S_1 against $[H_2O_2]_o^{-1}$ one obtains a line with slope $S_1' = k_A^{-1}$ and intercept $I_1' = k_C\, k_A^{-1}\, k_D^{-1}\, [MY]_o^{-1}$. Moreover, the plot of I_1 *vs.* $[H_2O_2]_o^{-1}$ is a line with slope $S_1'' = k_B\, k_A^{-1}\, k_D^{-1}\, [MY]_o^{-1}$ From the values of S_1', I_1' and S_1'' it is possible to obtain: $k_A = (S_1')^{-1}$; $k_C\, k_D^{-1} = I_1'\, (S_1')^{-1}\, [MY]_o$, and $k_B\, k_D^{-1} = S_1''\, (S_1')^{-1}\, [MY]_o$.

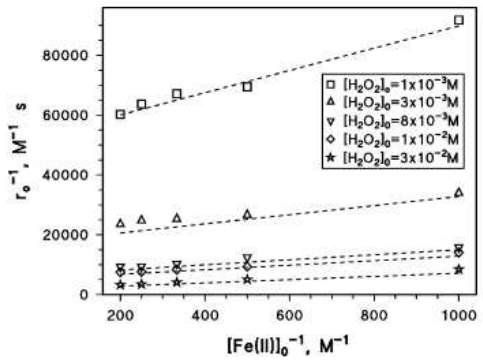

Figure 3. Reciprocal of the initial degradation rate of 10 μM MY as a function of the reciprocal of $[Fe(II)]_o$ (1-5 mM). $[H_2O_2]_o$ = 1-30 mM, pH 1.8 by H_2SO_4. Dashed lines: predictions of equation (13) with the data reported in Table 1, second column (MLR method).

In a similar way the plot of r_o^{-1} *vs.* $[H_2O_2]_o^{-1}$ is a line with slope $S_2 = \{k_B\, k_A^{-1}\, k_D^{-1}\, [MY]_o^{-1} + k_A^{-1}\, [Fe(II)]_o^{-1}\}$ and intercept $I_2 = \{k_C\, k_A^{-1}\, k_D^{-1}\, [MY]_o^{-1}\, [Fe(II)]_o^{-1}\}$. By plotting S_2 against $[Fe(II)]_o^{-1}$ one obtains a line with slope $S_2' = k_A^{-1}$ and intercept $I_2' = k_B\, k_A^{-1}\, k_D^{-1}\, [MY]_o^{-1}$. It is thus possible to obtain $k_A = (S_2')^{-1}$ and $k_B\, k_D^{-1} = I_2'\, (S_2')^{-1}\, [MY]_o$. Furthermore, by plotting I_2 *vs.* $[Fe(II)]_0^{-1}$ one obtains a line with slope $S_2'' = k_C\, k_A^{-1}\, k_D^{-1}\, [MY]_o^{-1}$. As a consequence, $k_C\, k_D^{-1} = S_2''\, (S_2')^{-1}\, [MY]_o$.

The experimental data allow two assessments of k_A, $k_B\, k_D^{-1}$ and $k_C\, k_D^{-1}$, which agree within 10% and are reported as average values in Table 1, first column (method = slope/intercept, $\mu \pm \sigma$). The initial degradation rates of MY as a function of $[Fe(II)]_o$ and $[H_2O_2]_o$ were also processed with a multiple linear regression (MLR) method using the Maple software, with equation (13) as the regression function. This data treatment allows a further assessment of k_A, $k_B\, k_D^{-1}$ and $k_C\, k_D^{-1}$ and the relevant data are reported in Table 1, second column (method = MLR). There is a very good agreement between the data obtained with the two methods (MLR and slope/intercept), the average of which is reported in Table 1, third column. The dashed lines in Figure 3 were obtained from equation (13) by introducing the data of k_A, $k_B\, k_D^{-1}$ and $k_C\, k_D^{-1}$ calculated by MLR. The agreement between experimental and predicted values is very good.

Table 1. Values of k_A, $k_B\ k_D^{-1}$, and $k_C\ k_D^{-1}$ obtained with two different methods (slope/intercept: see Figure 3 and the relevant discussion; MLR: multiple linear regression, with equation (13) as the regression function). The data in the third column are the averages of those in the first two columns. Errors = ±σ.

	Method		
	Slope/intercept	**MLR**	**Average**
$\mathbf{k_A}$	30.5±2.5	30.4±2.0	30.4±2.2
$\mathbf{k_B\ k_D^{-1}}$	(1.6±0.2)×10^{-2}	(1.6±0.1)×10^{-2}	(1.6±0.2)×10^{-2}
$\mathbf{k_C\ k_D^{-1}}$	(1.6±0.4)×10^{-3}	(1.3±0.4)×10^{-3}	(1.4±0.4)×10^{-3}

From the data of Table 1 one obtains $k_B\ k_C^{-1}$ = 11±5 (μ±σ). Under the hypothesis that the reactive species R is $^{\bullet}$OH, from the literature values of $k_{Ba} = 4.0 \times 10^8$ M^{-1} s^{-1} and $k_{Ca} = 2.7 \times 10^7$ M^{-1} s^{-1} [42] one gets $k_{Ba}\ k_{Ca}^{-1}$ = 14.8, which is inside the interval we have obtained (11±5). Therefore, the experimental data are compatible with $^{\bullet}$OH as the reactive species for MY degradation.

Reaction rate constant between MY and $^{\bullet}$OH. The value of k_{Da} (bimolecular rate constant between MY and $^{\bullet}$OH in aqueous solution) can be evaluated independently upon addition of 2-propanol as $^{\bullet}$OH scavenger (with rate constant of 1.9×10^9 M^{-1} s^{-1} at 25°C [42]), under the assumption that the key reactant is the hydroxyl radical. In the presence of 2-propanol a reaction needs to be added to the kinetic model:

$$\text{2-Propanol} + \text{R} \rightarrow \text{products} \qquad [k_E] \qquad (14)$$

The application of the steady-state approximation to [R] yields:

$$\left(r_o^P\right)^{-1} = r_o^{-1} + \frac{k_E}{k_A \cdot k_{Da} \cdot [\text{Fe(II)}]_o \cdot [H_2O_2]_o \cdot [\text{MY}]_o} \cdot [2-\text{propanol}]_o \qquad (15)$$

where r_o^P is the initial degradation rate measured in the presence of 2-propanol and r_o that measured in its absence. The expression for r_o^{-1} is reported in equation (13). Equation (15) implies that the plot of $(r_o^P)^{-1}$ *vs.* [2-propanol]$_o$ is linear. Such a plot is reported in Figure 4 in the presence of 10 μM MY, 1 mM Fe(II) and 1.5 mM H_2O_2, varying [2-propanol]$_o$ in the range of 0.14-1.00 mM.

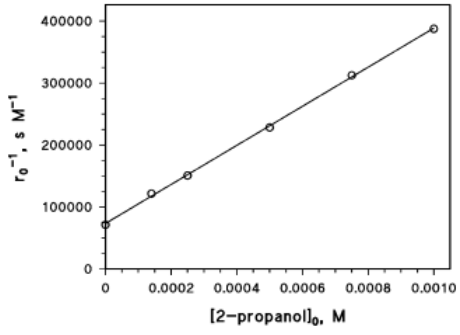

Figure 4. Reciprocal of the initial degradation rate of 10 μM MY as a function of [2-propanol]$_o$. [Fe(II)]$_o$ = 1 mM, [H_2O_2]$_o$ = 1.5 mM, pH 1.8 by H_2SO_4, reaction temperature 25°C. The regression line is also reported.

The plot of r_o^{-1} *vs.* [2-propanol]$_o$ is a line with slope S_3 = (3.15±0.04)×10^8 M^{-2} s and intercept I_3 = (7.33±0.21)×10^4 M^{-1} s. From the slope it is possible to assess $k_{Da} = k_E\ \{S_3\ k_A\ [\text{Fe(II)}]_o\ [H_2O_2]_o\ [\text{MY}]_o\}^{-1}$. Using the value $k_E = 1.9 \times 10^9$ M^{-1} s^{-1} for reaction between 2-propanol and $^{\bullet}$OH,[42] one obtains k_{Da} = (1.3±0.1)×10^{10} M^{-1} s^{-1} as the reaction rate constant of MY with $^{\bullet}$OH. This value is very similar to those reported for the reaction between $^{\bullet}$OH and other azo-dyes (Acid Blue 40, 1.2×10^{10} M^{-1} s^{-1}; Acid Blue 74, 1.8×10^{10} M^{-1} s^{-1}).[42] The data reported so far indicate that the kinetics of MY degradation by the Fenton reagent is compatible with an $^{\bullet}$OH-initiated process (mechanism A). Mechanism B (through the ferryl ion) could also be compatible, although unlikely, by assuming that FeO^{2+} reacts with almost the same rate constants of $^{\bullet}$OH with Fe(II), H_2O_2 and 2-propanol.

Quantification of $^{\bullet}$OH and ferryl generation. It is interesting to observe that Table 1 reports a k_A value (30.4±2.2 M^{-1}s^{-1}) that is lower than those reported in the literature for Fe^{2+} + H_2O_2 (ranging in the interval 50-65 M^{-1}s^{-1}).[17,37,39] Note that the literature values have been obtained by measuring the disappearance rate of either Fe(II) or H_2O_2, while we have monitored the transformation of MY and estimated as a consequence the generation rate of the key reacting species R. The disagreement between the value of k_A calculated here and those reported in the literature suggests that Fe(II) disappears at a higher rate compared to the formation of the key reacting species. This issue has already been described in the literature [17] and might be due to the formation of both ferryl and $^{\bullet}$OH in separate but parallel processes as depicted in reactions (5-10). This possibility is supported by molecular dynamic calculations,[43] which showed that as H_2O_2 is coordinated to Fe(II) or is entering the coordination shell, the oxygen-oxygen bond breaks to form Fe(III) (actually, $[(H_2O)_5Fe^{III}OH]^{2+}$) and a very short-lived $^{\bullet}$OH radical. The hydroxyl radical could either react with a water ligand to form $[(H_2O)_4Fe^{IV}(OH)_2]^{2+}$ and a water molecule, producing the ferryl ion in a second step by dehydration, or abstract hydrogen from the OH^- ligand, directly producing ferryl. Moreover, other evidence has accumulated in favour of the contemporary formation of both species in the Fenton reaction.[8-14]

The application of the steady-state approximation to [$^{\bullet}$OH], [FeO^{2+}] and [{Fe^{2+}-H_2O_2}], when both reaction pathways are included (in this case, mechanisms A and B are considered together) yields an expression for the initial MY transformation rate ($r_o = k_{Da}\ [^{\bullet}\text{OH}]_o\ [\text{MY}]_o + k_{Db}\ [FeO^{2+}]_o\ [\text{MY}]_o$, equation (16)) that is incompatible with the linearisation reported in Figure 3.

The linearisation of $1/r_o$ *vs.* $1/[X]_o$, where X = H_2O_2 or Fe^{2+}, is possible if only one MY degradation process (involving either $^{\bullet}$OH or FeO^{2+}) is operational, as already deduced. Since for other organic amines and azo dyes the reaction with $^{\bullet}$OH is not only possible, but also quite fast, we must conclude that MY reacts preferentially with $^{\bullet}$OH and that the reaction with ferryl plays a negligible role in MY degradation.

$$\frac{1}{r_o} = \frac{(k_2 + k_{3a} + k_{3b})(k_{Bb}[Fe^{2+}]_o + kC_{Cb}[H_2O_2]_o + k_{Db}[MY]_o) \times (k_{Ba}[Fe^{2+}]_o + k_{Ca}[H_2O_2]_o + k_{Da}[MY]_o)}{k_1[H_2O_2]_o[Fe^{2+}]_o[MY]_o\{(k_{Da}k_{3a}k_{Bb} + k_{Db}k_{3b}k_{Ba})[Fe^{2+}]_o + (k_{Da}k_{3a}k_{Cb} + k_{Db}k_{3b}k_{Ca})[H_2O_2]_o + (k_{3a} + k_{3b})k_{Db}k_{Da}[MY]_o\}} \qquad (16)$$

Therefore, assuming that $r_o = k_{Da}\,[^{\bullet}OH]_o\,[MY]_o$, a rate expression almost identical to equation (13) is obtained, with the only difference that k_A assumes a different meaning:

$$k_A = \frac{k_1 \cdot k_{3a}}{k_2 + k_{3a} + k_{3b}} \qquad (17)$$

By so doing, the relevant kinetic model is based on reactions (5,6,7a,8a,9a,10a,7b,8b,9b), excluding reaction (10b). In the steady-state approximation, however, reactions (8b,9b) have no influence on the transformation rate of MY. The model yields the following expression for the bimolecular rate constant k^{Fe}_A between Fe(II) and H_2O_2 in reactions (5-7):

$$k^{Fe}_A = \frac{k_1(k_{3a} + k_{3b})}{k_2 + k_{3a} + k_{3b}} \qquad (18)$$

This result justifies the observed difference between the literature value for k^{Fe}_A (52.4 $M^{-1}s^{-1}$ [39], 53.0 $M^{-1}s^{-1}$ [37]) and our data (k_A = 30.4 ± 2.2 $M^{-1}s^{-1}$). The ratio of $k_A/k^{Fe}_A = k_{3a} / (k_{3a} + k_{3b}) = 0.58$ (for k^{Fe}_A = 52.8 $M^{-1}s^{-1}$) implies that ~60% of the complex {Fe^{2+}-H_2O_2} would produce $^{\bullet}OH$ radicals, whilst the remaining ~40% would form species that do not react at an appreciable rate with MY under the adopted conditions. Because the k_A/k^{Fe}_A ratio is independent on k_D, it follows that for any Fenton system at the studied pH value (1.8) the kinetic pathways have the same k_A/k^{Fe}_A ratio. This finding helps explaining the disagreement between the reaction rate of Fe(II) and H_2O_2 and the generation rate of $^{\bullet}OH$.[17]

Degradation of dichloroanilines with the Fenton reagent

The Fenton degradation of dichloroanilines (2,4-DCA and 3,4-DCA, hereafter both indicated as DCA, used at 0.8 mM initial concentration) was studied in aqueous solution at pH 2.0 by H_2SO_4. Under these conditions both substrates are protonated.[44] Figure 5 reports that DCA degradation in the presence of 0.2-0.6 mM Fe(II) and 1-3 mM H_2O_2 has a very fast initial step (ferrous step, triggered by $Fe^{2+} + H_2O_2$) that goes to completion within 1 min reaction time. Afterwards the kinetic regime changes to a slower ferric step, dominated by Fe(III) reduction. Considering that we used [Fe(II)] < $[H_2O_2]$, based on the above kinetic analysis of the ferrous step we assume that the ending of this step is due to the complete consumption of Fe(II).

If (as it is reasonable) the rate constant between DCA and $^{\bullet}OH$ is of the same order of magnitude as that of MY, the initial concentration value of DCA (0.8 mM) implies that the competitive $^{\bullet}OH$ reactions with Fe(II) and H_2O_2 are negligible. Within this context one obtains that the relative transformation of DCA at the end of the ferrous step is:

$$\frac{\Delta[DCA]}{[DCA]_o} = \beta = \frac{k_A}{k^{Fe}_A} \cdot \frac{\Delta[Fe(II)]}{[DCA]_o} = \frac{k_A}{k^{Fe}_A} \cdot \frac{[Fe(II)]_o}{[DCA]_o} \qquad (19)$$

(for k_A and k^{Fe}_A see equations (17) and (18) and the relative discussion; the use of $\Delta[Fe(II)] = [Fe(II)]_o$ implies that Fe(II) is completely consumed in the ferrous step).

Based on data reported in Figure 5A/B, the plot of β *vs.* $[Fe(II)]_o/[DCA]_o$ is a line with slope k_A/k^{Fe}_A = 0.66 (Figure 6). This is fully consistent with the value of 0.58 already found in the case of MY and constitutes additional evidence that the reaction between Fe(II) and H_2O_2 yields both $^{\bullet}OH$ (about 60% at pH 2) and FeO^{2+} (about 40%), with $^{\bullet}OH$ alone contributing to substrate degradation in the present case.

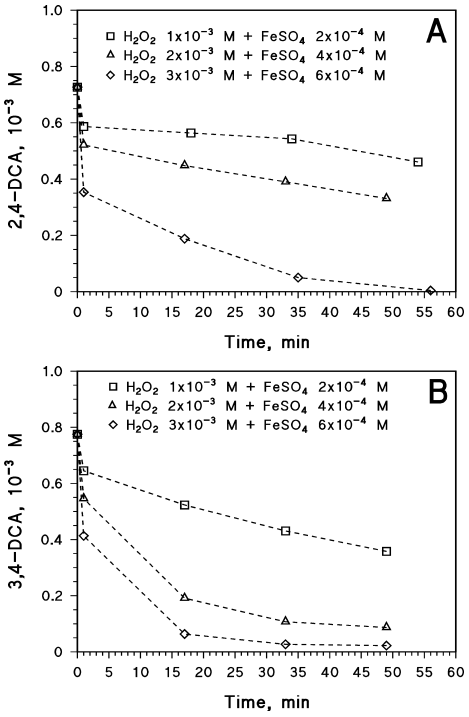

Figure 5. (A) Degradation of 0.8 mM 2,4-DCA with the Fenton reagent in aqueous solution (the values of $[Fe(II)]_o$ and $[H_2O_2]_o$ are indicated on the Figure). pH 2.0 by addition of H_2SO_4.
(B) Degradation of 0.8 mM 3,4-DCA with the Fenton reagent in aqueous solution (the values of $[Fe(II)]_o$ and $[H_2O_2]_o$ are indicated on the Figure). pH 2.0 by addition of H_2SO_4.

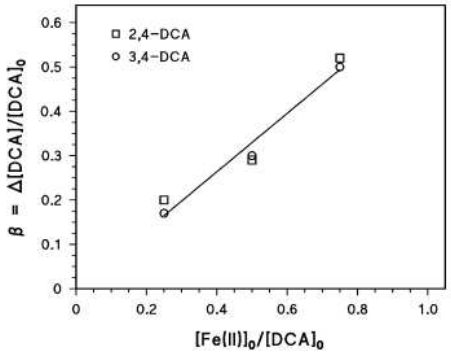

Figure 6. Plot of $\beta = \Delta[DCA]/[DCA]_o$ *vs.* $[Fe(II)]_o/[DCA]_o$, based on the data of Figure 5. Slope = k_A/k^{Fe}_A = 0.66. Note that DCA = 2,4-DCA or 3,4-DCA.

Among the intermediates of the Fenton degradation of 2,4-DCA it was possible to detect the corresponding phenol (2,4-DCP), the 2-chloro-1,4-benzoquinone (CBQ) and a trichloroaniline (2,4,6-TCA). Ammonium and chloride were also formed. The formation of 2,4-DCP would occur upon deamination of 2,4-DCA, which also yields ammonium, while no nitrate could be detected in the

system. A similar result has been obtained by Bossmann et al. in the case of 2,4-dimethylaniline.[3] The intermediate CBQ is most likely formed upon oxidative dechlorination of 2,4-DCP, presumably initiated by attack of $^{\bullet}OH$ on the carbon atom bound to chlorine. In this way, one of the two chlorine atoms initially present on the substrate would be transformed into a chloride ion.

When 2,4-DCA disappears, about 70% of organic nitrogen is transformed into ammonium and 35% of organic chlorine into chloride. The low generation of chloride can be accounted for if the transformation of organic chlorine into chloride is faster for one of the two Cl atoms of 2,4-DCA. This would be consistent with the detection of CBQ as intermediate. Another possible contribution to the low chloride generation comes from the formation of 2,4,6-TCA. This compound is likely to be formed upon chlorination of 2,4-DCA in the presence of $Cl^{\bullet}/Cl_2^{-\bullet}$, as $Cl_2^{-\bullet}$ is a chlorinating agent.[45] The chlorine-containing radicals can be produced upon oxidation of chloride by $^{\bullet}OH$:[46]

$$^{\bullet}OH + Cl^- \rightleftharpoons {}^{\bullet}ClOH^- \qquad [K_{eq,20} = 0.70\ M^{-1}] \quad (20)$$

$$^{\bullet}ClOH^- + H^+ \rightleftharpoons Cl^{\bullet} + H_2O \qquad [K_{eq,21} = 1.6\times10^{7}] \quad (21)$$

$$Cl^{\bullet} + Cl^- \rightarrow Cl_2^{-\bullet} \qquad (22)$$

In this way, 2,4,6-TCA would constitute a reservoir of organic chlorine and organic nitrogen, slowing down the generation of both chloride and ammonium.

Furthermore, the Fenton degradation of 3,4-DCA yields 3,4-DCP, ammonium, and chloride.

Conclusions

The dark Fenton process involving Fe(II) + H_2O_2 consists of two regimes, a fast ferrous one that is triggered by the reaction of Fe^{2+} + H_2O_2 and a slow ferric one that is dominated by the reduction of Fe(III). The ferrous regime was studied with the stopped-flow technique, using methyl yellow (MY) as a substrate. A kinetic model that is able to account for all the observed results requires that the reaction between Fe(II) and H_2O_2 produces both $^{\bullet}OH$ (~60% yield) and another species, possibly the ferryl ion (FeO^{2+}) (~40% yield) in parallel processes, with ferryl reacting with MY at a negligible rate. The experimental data are consistent with the degradation of MY taking place upon reaction with $^{\bullet}OH$, with rate constant k_{Da} = (1.3±0.1)×10^{10} M^{-1} s^{-1} at 25°C. The hypothesis of the formation of both $^{\bullet}OH$ and FeO^{2+}, with $^{\bullet}OH$ alone being reactive, also accounts for the degradation of dichloroanilines (2,4-DCA and 3,4-DCA) in the ferrous step. The kinetic model we proposed might be a way out of a long-lasting controversy concerning the Fenton reagent, and it also allowed the quantification of the formation yields of the reactive species.

Notes and references

[a] Dipartimento di Chimica, Università di Torino, Via P. Giuria 5, 10125 Torino, Italy.*http://www.environmentalchemistry.unito.it*. Phone +39-011-6705296. Fax +39-011-6705242.
E-mail: *claudio.minero@unito.it*; *davide.vione@unito.it*.

1 C. Walling, *Acc. Chem. Res.*, 1975, **8**, 125.
2 D. T. Sawyer, C. Kang, A. Llobet and C. Redman, *J. Am. Chem. Soc.*, 1993, **115**, 5817.
3 S. H. Bossmann, E. Oliveros, S. Göb, S. Siegwart, E. P. Dahlen, L. Payawan Jr., M. Straub, M. Wörner and A. M. Braun, *J. Phys. Chem. A*, 1998, **102**, 5542.
4 D. T. Sawyer, A. Sobkowiak and T. Matsushuta, *Acc. Chem. Res.*, 1996, **29**, 409.
5 F. Gozzo, *J. Mol. Catal. A: Chem.*, 2001, 171, 1.
6 I. Yamazaki and L. H. Piette, *J. Am. Chem. Soc.*, 1991, **113**, 7588.
7 M. D. Paciolla, S. Kolla and S. A. Jansen, *Adv. Environ. Res.* 2002, **7**, 169.
8 J. T. Groves, *J. Inorg. Biochem.*, 2006, **100**, 434.
9 J. Bautz, M. R. Bukowski, M. Kerscher, A. Stubna, P. Comba, A. Lienke, E. Munck, and L. Que, *Angew. Chem. Intern. Ed.*, 2006, **45**, 5681.
10 L. Deguillaume, M. Leriche, and N. Chaurneliac, *Chemosphere*, 2005, **60**, 718.
11 R. Gonzales-Olmos, F. Holzer, F. D. Kopinke, and A. Georgi, *Appl. Catal. A: Gen*., 2011, **398**, 44.
12 K. Barbusinski, *Ecol. Chem. Engineer*., 2009, **16**, 347.
13 O. Pestovsky, S. Stoian, E. L. Bominaar, X. P. Shan, E. Munck, L. Que, and A. Bakac, *Angew. Chem. Intern. Ed.*, 2005, **44**, 6871.
14 N. Yamamoto, N. Koga, and M. Nagaoka, *J. Phys. Chem. B*, 2012, **116**, 14178.
15 S. Y. Pang, J. Jiang, and J. Ma, *Environ. Sci. Technol*., 2011, **45**, 307.
16 H. Bataineh, O. Pestovsky, and A. Bakac, *Chem. Sci*., 2012, **3**, 1594.
17 H. Gallard, J. De Laat and B. Legube, *New J. Chem.*, 1998, **22**, 263.
18 J. De Laat and H. Gallard, *Environ. Sci. Technol.*, 1999, **33**, 2726.
19 L. W. Chen, J. Ma, X. C. Li, J. Zhang, J. Y. Fang, Y. H. Guan and P. C. Xie, *Environ. Sci. Technol*., 2011, **45**, 3925.
20 O. Legrini, E. Oliveros and A. M. Braun, *Chem. Rev.*, 1993, **93**, 671.
21 H. Gallard and J. De Laat, *Chemosphere*, 2001, **42**, 405.
22 M. Kitis, C. D. Adams and G. T. Daigger, *Water Res.*, 1999, **33**, 2561.
23 A. Hadasch, A. Sorokin, A. Rabion and B. Meunier, *New J. Chem*., 1998, **22**, 45.
24 F. Chen, W. Ma, J. He and J. Zhao, *J. Phys. Chem. A*, 2002, **106**, 9485.
25 S. Esplugas, J. Gimenez, S. Contreras, E. Pascual and M. Rodriguez, *Water Res.*, 2002, **36**, 1034.
26 K. D. Zoh and M. K. Stenstrom, *Water Res.*, 2002, **36**, 1331.
27 R. J. Watts, P. C. Stanton, J. Howsawkeng and A. L. Teel, *Water Res.*, 2002, **36**, 4283.
28 M. E. Lindsey and M. A. Tarr, *Water Res.*, 2000, **34**, 2385.
29 M. E. Lindsey and M. A. Tarr, *Chemosphere*, 2000, **41**, 409.
30 S. H. Gau and F. S. Chang, *Water Sci. Technol*. 1996, **34**, 455.
31 F. Chen, J. J. He, J. C. Zhao and J. C. Yu, *New J. Chem.*, 2002, **26**, 336.
32 M. Perez, F. Torrades, X. Domenech and J. Peral, *Water Res.*, 2002, **36**, 2703.
33 M. Ravina, L. Campanella and J. Kiwi, *Water Res.*, 2002, **36**, 3553.
34 P. Mazellier and B. Sulzberger, *Environ. Sci. Technol.*, 2001, **35**, 3314.
35 B. Gozmen, M. A. Oturan, N. Oturan and O. Erbatur, *Environ. Sci. Technol*., 2003, **37**, 3716.
36 C. Minero, M. Lucchiari, D. Vione and V. Maurino, *Environ. Sci. Technol*., 2005, **39**, 8936.
37 W. G. Barb, J. H. Baxendale, P. George and K. R. Hargrave, *Trans. Faraday Soc.*, 1951, **47**, 462.
38 M. L. Kremer, *Phys. Chem. Chem. Phys.*, 1999, **1**, 3595.
39 M. L. Kremer, *J. Phys. Chem. A*, 2003, **107**, 1734.
40 C. Minero, P. Pellizzari, V. Maurino, E. Pelizzetti and D. Vione, *Appl. Catal. B: Environ*., 2008, **77**, 308.
41 M. L. Kremer, *J. Inorg. Biochem.*, 2000, **78**, 255, and the erratum at *ibidem*, 2000, **81**, 325.
42 G. V. Buxton, C. L. Greenstock, W. P. Helman and A. B. Ross, *J. Phys. Chem. Ref. Data*, 1988, **17**, 1027.
43 B. Ensing, F. Buda, P. E. Blochl and E. J. Baerends, *Phys. Chem. Chem. Phys.*, 2002, **4**, 3619.
44 A. E. Martell, R. M. Smith and R. J. Motekaitis, *Critically selected stability constants of metal complexes database*. Version 4.0, 1997.
45 M. Brigante, M. Minella, G. Mailhot, V. Maurino, C. Minero, D. Vione, *Chemosphere*, in press. DOI: http://dx.dox.org/10.1016/j.chemosphere.2013.09.098.
46 G. G. Jayson, B. J. Parsons and A. J. Swallow, *J. Chem. Soc. Faraday I*, 1973, 1597.